

Wind Pressure and Velocity Distributions around an Irregular Plan-shaped Building

Tuğba İnan Günaydin^{1*}

¹ Department of Architecture, Faculty of Architecture, Niğde Ömer Halisdemir University, Bor Street, 51240 Niğde, Turkey

* Corresponding author, e-mail: tinan@ohu.edu.tr

Received: 14 July 2021, Accepted: 14 July 2022, Published online: 25 July 2022

Abstract

Wind is a significant architectural design parameter to be considered during the initial phase of the design stage. However, there are very few studies on the wind behaviour of buildings in the architectural field. Understanding the behaviour of buildings under wind loads is significant to developing solutions at every stage of the design phase.

This study presents the numerical examination of wind pressure distributions on U-plan-shaped buildings with four different depth ratios of 0.5, 1, 2, and 4 over a wind incidence angle of 0°. Models were examined with 2 and 5 m/s wind velocity values. This study aims to examine the effect of depth ratios and wind velocity values on an irregular building. Wind pressure distributions around models, wind velocity distributions, wind flows and streamlines have been comprehensively evaluated.

As a result of the studies, it has been observed that according to the wind pressure distributions around building models, when the U1, U2 and, U7, U8 models are compared, it can be seen that the negative pressure difference decreases slightly as the depth ratio decreases. Furthermore, as the wind velocity increased, the negative pressure difference decreased. It was observed that there was no significant difference in terms of positive pressure values. Moreover, it was observed that from the height level of $H/3$ to $2H/3$, the vortex region decreases. This vortex area is more significant in the U7 model, which has a depth ratio of 0.5. The vortex area increases as the depth ratio decreases.

Keywords

wind, irregular plan, computational fluid dynamics (CFD), pressure distributions

1 Introduction

Wind is one of the significant loads to be considered at every stage of the architectural design phase. It is a significant architectural design component, and there is increasing interest in analysing wind load effects on buildings from an engineering perspective. However, understanding the behaviour of buildings under wind load is also significant in the architectural field.

There are various studies in the literature related to the analysis of wind flow mechanisms and understanding of wind characteristics on buildings (Al-Najjar and Al-Azhari, 2021; Bhattacharya and Dalui, 2020; Jendzelovsky and Antal, 2021; Mallick et al., 2020; Paul and Dalui, 2021). Significantly, the wind behaviour of irregular plan-shaped buildings is a significant subject to be analysed. Some of the irregular forms were studied by researchers in the literature (Bhattacharyya and Dalui, 2018; Chakraborty et al., 2014; Gomes et al., 2005;

İnan, 2021; Li et al., 2020; Mallick et al., 2019; Mukherjee et al., 2014; Sanyal and Dalui, 2021).

There are very few studies on the wind behaviour of buildings in the architectural field. Moreover, the behaviour of the buildings under wind velocities has not been generally understood by architectural students. Understanding the behaviour of buildings under wind loads is significant to developing solutions at every stage of the design phase. In this study, wind behaviour in buildings is evaluated from an architectural point of view. This study presents the numerical examination of wind pressure distributions on U-plan-shaped buildings with four different depth ratios of 0.5, 1, 2, and 4 over a wind incidence angle of 0°. Models were examined with 2 and 5 m/s wind velocity values. This study aims to examine the effect of depth ratios and wind velocity values on the wind behaviour of an irregular building.

2 Research methodology

In this study, the Computational Fluid Dynamics (CFD) package of ANSYS FLUENT 20.0 is used for the analysis. CFD. In accordance with suggestions in the literature (Franke, 2006; Tominaga et al., 2008), the computational domain used for the analysis in this study is presented in Fig. 1. While $5H$ is taken for the top, inlet and side walls, $15H$ is taken from the outlet in this study. In meshing, grid quality and quantity ascertain computation time and results. In this study, a hexahedra grid type is chosen to predict results.

This study uses velocity inlet as inlet boundary with wind and turbulence quantities. Outlet is modelled as out-flow boundary, side walls and top wall have symmetrical boundary conditions, and ground (bottom wall) has no-slip boundary conditions. These boundary conditions are used during the numerical simulation in ANSYS FLUENT 20.0. A realisable $k-\epsilon$ turbulent model is performed in the analysis. The SIMPLE algorithm of Patankar was used to solve the pressure-velocity coupling (Patankar, 1980). Second-Order Upwind Scheme was used for the convection terms and the viscous terms of the governing equations. In the analyses, for all of the transport parameters, the convergence criterion has been defined as 10^{-7} .

2.1 Models

Four U-shaped buildings with the same height, width and wing length but having different depth plan ratios were analysed by applying the Computational Fluid Dynamics (CFD) package of ANSYS 20. For this purpose, wind pressure distributions on and around U-plan-shaped buildings were analysed for the wind velocity value of 2 m/s and 5 m/s over a wind incidence angle of 0° . While U1, U3, U5 and U7 models were exposed to 2 m/s, the others were exposed to 5 m/s wind velocity.

Models could be denoted as U1 to U8 according to depth ratio (DR) and wind velocity values. Moreover, other particular information about the models is given in Fig. 2 and Table 1. Depth ratio (DR) is determined as the ratio of building wing length to the length between building wings. The depth ratios calculated in the models are 0.5, 1, 2, and 4. All surfaces are coded with letters as shown in Fig. 2. All models are designed as having a building height of 30 m. While the models coded as U1, U3, U5 and U7 were exposed to 2 m/s wind velocity, the others were under 5 m/s wind velocity. These wind velocities were chosen based on the wind map of Niğde/Turkey, and average and minimum velocity values were used in the study analysis.

3 Discussion and results

In this study, ANSYS Fluent Computational Fluid Dynamics (CFD) software 20.0 package program is used to analyse wind pressure and velocity distributions around shaped-plan-shaped buildings. The results from the analysis are examined comprehensively in this part.

In the study, wind pressure coefficients are sliced at the height level of $2H/3$, $H/2$ and $H/3$, as shown on the U4 model – Fig. 3. The aim is to examine wind characteristics around U-plan-shaped buildings with different depth ratios and height levels.

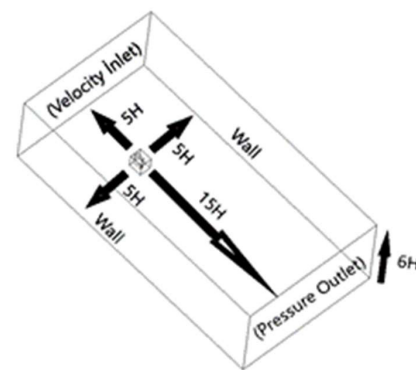


Fig. 1 Computational domain

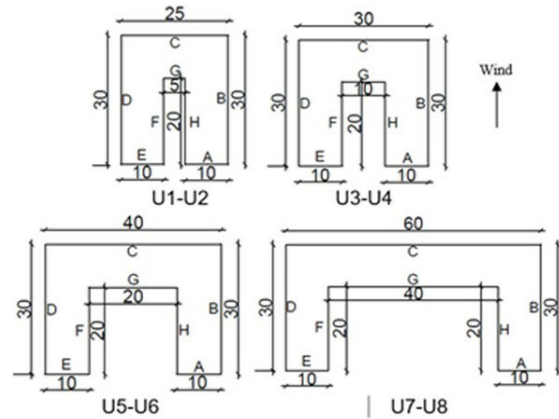


Fig. 2 Building models

Table 1 Parameters and computational domain dimension

Model	DR	Wind (m/s)	Computational Domain (m)
			X × Y × Z
U1	4	2	325 × 630 × 180
U2	4	5	325 × 630 × 180
U3	2	2	330 × 630 × 180
U4	2	5	330 × 630 × 180
U5	1	2	340 × 630 × 180
U6	1	5	340 × 630 × 180
U7	0.5	2	360 × 630 × 180
U8	0.5	5	360 × 630 × 180

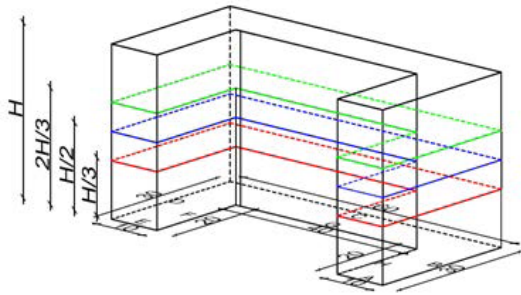


Fig. 3 Horizontal lines for pressure coefficients

3.1 Wind Pressure Distributions around building models

Wind pressure distributions around shaped-shaped building models were analysed for different wind velocity and depth ratio (DR) conditions. All models were evaluated at the height of $H/3$, $H/2$, and $2H/3$ levels. Graphs of the selected models were presented to avoid excessive graphing when evaluating the study. In shaped-shaped models, positive pressure values were observed on windward surfaces (A, E, G). Moreover, negative pressure values were noticed on leeward (C) and especially on side surfaces (B, D).

In the U1 model, while the positive pressure values around the buildings decrease from $H/3$ level to $2H/3$ height level, negative pressure values decrease from $H/3$ to $H/2$ height level (Fig. 4). After, it started to increase to the $2H/3$ level. U2 shows similar behaviour as U1. However, considerable high-pressure values were noticed around the buildings due to the high wind velocity value (Fig. 5). When the models U1 and U7, which were exposed to 2 m/s wind velocity, were compared, it was observed that there was no significant difference in terms of positive pressure values. However, significant differences were observed in negative pressure values. It was observed that the negative pressure values around the U7 model – 0.5 depth ratio – are approximately twice that of the U1 model with a depth ratio of 4 (Fig. 6).

When the models U2 and U8 that were exposed to 5 m/s wind velocity were compared, it was observed that there was no significant difference in terms of positive pressure values. However, significant differences were observed in negative pressure values. The negative pressure values around the U8 model – depth ratio of 0.5 – are approximately 1.5 times that of the U2 model with a depth ratio of 4 (Fig. 7).

When the models U1 and U2, which have the same depth ratio of 4, were compared, it was observed that positive pressure values around the U2 model, which was

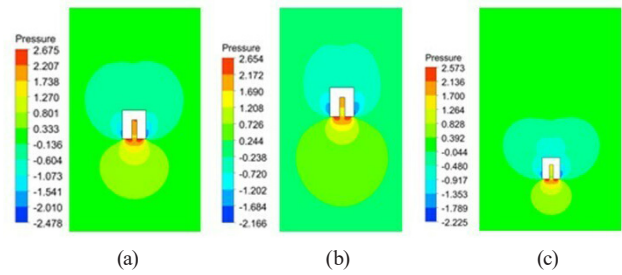


Fig. 4 Wind pressure distributions around buildings for U1 (DR:4, wind velocity 2 m/s); (a) $z = H/3$, (b) $z = H/2$, (c) $z = 2H/3$

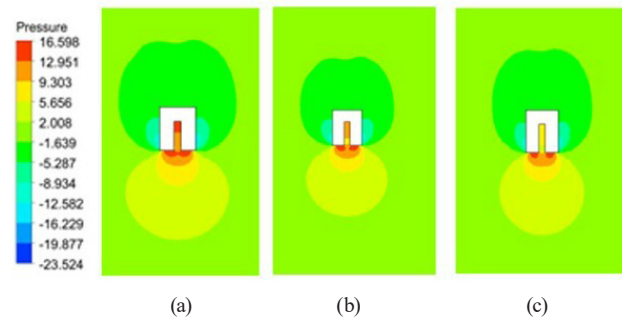


Fig. 5 Wind pressure distributions around buildings for U2 (DR:4, wind velocity 5 m/s); (a) $z = H/3$, (b) $z = H/2$, (c) $z = 2H/3$

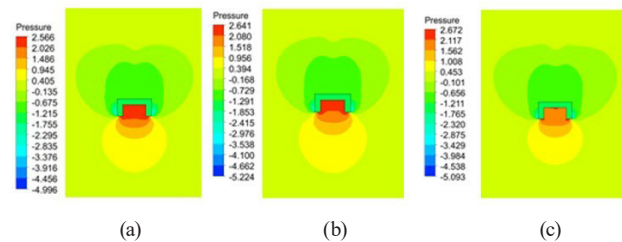


Fig. 6 Wind pressure distributions around buildings for U7 (DR:0.5, wind velocity 2 m/s); (a) $z = H/3$, (b) $z = H/2$, (c) $z = 2H/3$

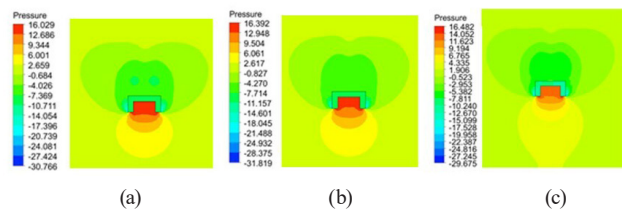


Fig. 7 Wind pressure distributions around buildings for U8 (DR:0.5, wind velocity 5 m/s); (a) $z = H/3$, (b) $z = H/2$, (c) $z = 2H/3$

exposed to 5 m/s wind velocity, are approximately eight times that of the U1 model. Besides, negative pressure values are about 11 times greater than U1.

On the other hand, when the models U7 and U8, which have the same depth ratio of 0.5, were compared, it was observed that positive pressure values around the U8 model, which was exposed to 5 m/s wind velocity, are approximately eight times that of the U7 model. Besides, negative pressure values are about eight times greater than U7.

When the U1, U2 and, U7, U8 models are compared, it is seen that the negative pressure difference decreases slightly as the depth ratio decreases. Besides, as the wind velocity increased, the negative pressure difference decreased.

3.2 Velocity distributions

Figs. 8 and 9 show the streamlines on the horizontal plane of $H/3$ and $2H/3$ height levels for wind directions of 0° for the U1 and U7 models. It was noticed that wind flows sharply away from the windward surface (A and E) nearest to the side surfaces. The flow separation and acceleration of flow are noticeable on the outside corners, and wind flow reverses just behind these corners. Two similar vortices appear in the wake region of the U-shaped models. Significant negative pressures were noticed on and around side surfaces and the leeward surface.

Moreover, the vortex region gets smaller from the height level of $H/3$ to $2H/3$. This vortex area is more significant in the U7 model, which has a depth ratio of 0.5. The vortex area gets larger as the depth ratio decreases.

Wind flows around shaped-shaped models were presented in Figs. 10–13. At the height of $z = H/3$, turbulent flow is observed on the side surfaces of all models. Moreover, the velocity in the track zone decreases and reverse flow zones are formed. Maximum velocity occurs on the side surfaces of buildings. It is observed that the maximum velocity region on the side surfaces of the models expanded with

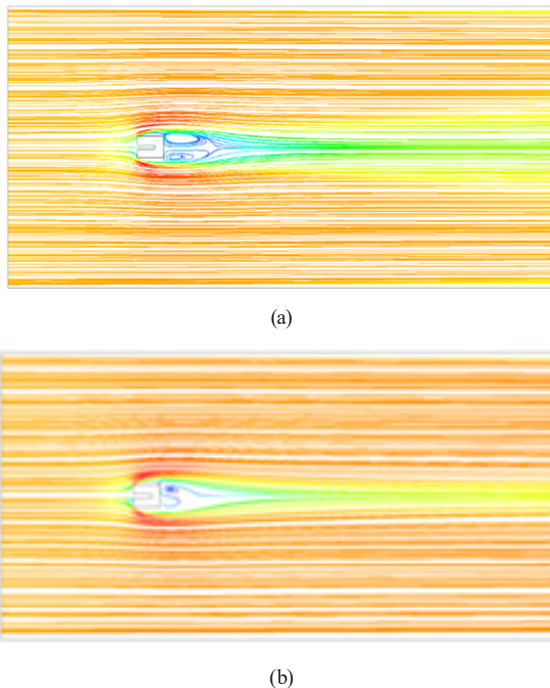


Fig. 8 Streamlines around the U1-shaped model: (a) $z = H/3$, (b) $z = 2H/3$

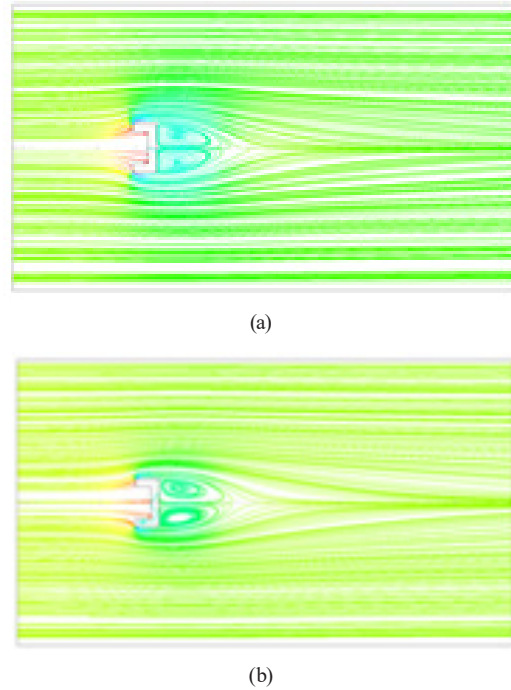


Fig. 9 Streamlines around the U7-shaped model: (a) $z = H/3$, (b) $z = 2H/3$

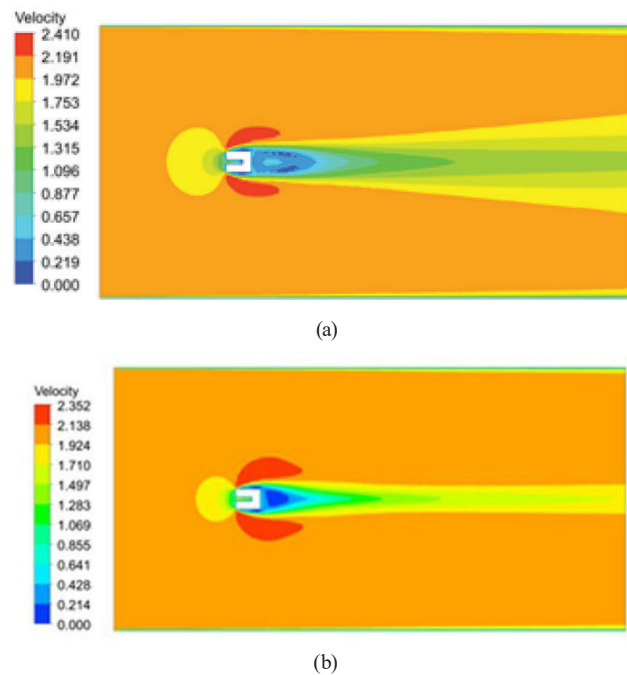


Fig. 10 Velocity distributions around U1 model; (a) $z = H/3$, (b) $z = 2H/3$

increasing height in all models. In the trace region, velocity decreases in all models in the velocity region. However, as the height of the model decreases, the velocity drops in the track zone increases. When the models of U1 and U2, which were exposed to the same depth ratio and different wind velocities, were compared, it was noticed that the U2 model had considerable high-pressure values. Moreover, while the pressure areas on the side surfaces of the U2

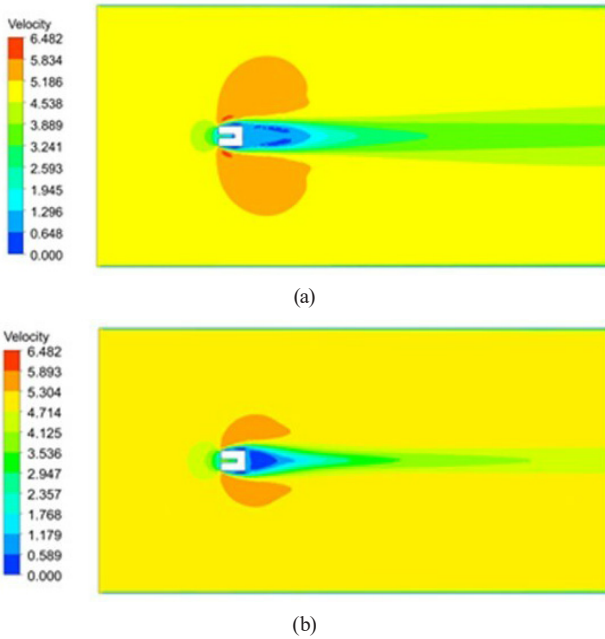


Fig. 11 Velocity distributions around U2 model; (a) $z = H/3$, (b) $z = 2H/3$

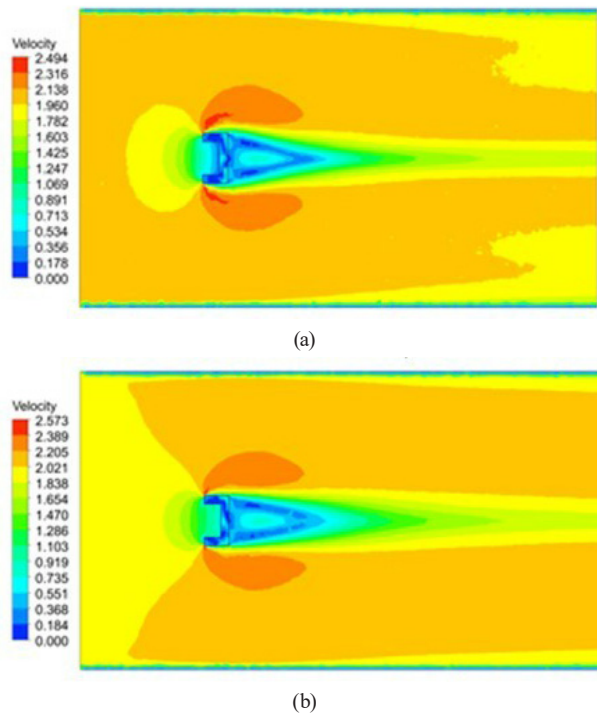


Fig. 12 Velocity distributions around U7 model; (a) $z = H/3$, (b) $z = 2H/3$

and U8 models, which are exposed to high wind velocity, decrease with height, an increasing trend is observed for U1 and U7, which are exposed to low wind velocity.

4 Conclusions

This paper presented the numerical examination of wind pressure and velocity distributions around irregular U-plan-shaped models having different depth ratios and wind

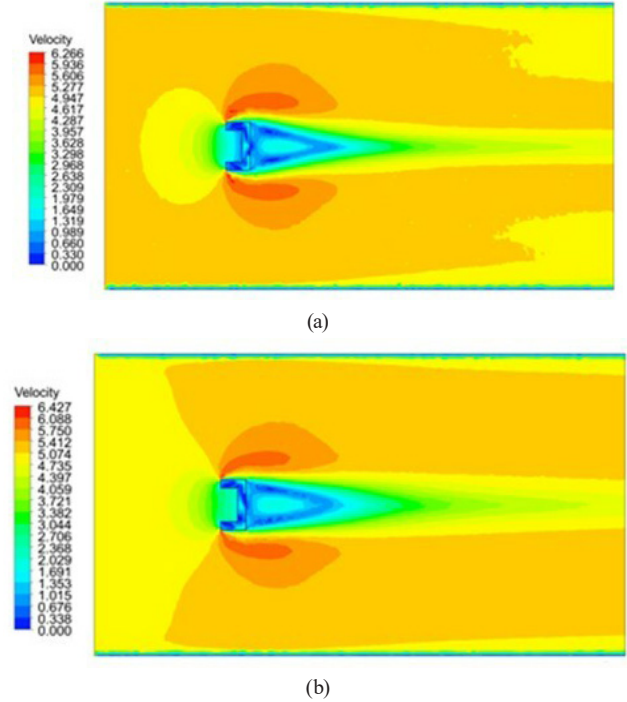


Fig. 13 Velocity distributions around U8 model; (a) $z = H/3$, (b) $z = 2H/3$

velocities. While U1, U3, U5 and U7 models were exposed to 2 m/s, the others were exposed to 5 m/s wind velocity. The models U1 and U2 have the same depth ratio of 4.00. U3 and U4 have the same depth ratio of 2.00, U5 and U6 have the same depth ratio of 1.00 and U7 and U8 have the same depth ratio of 0.50. This study aimed to examine the effect of depth ratios and wind velocities on wind pressure distributions around all models. With this aim, the ANSYS Fluent 20.0 Computational Fluid Dynamics (CFD) software program was used for the numerical analysis. The flow was considered steady, fully turbulent and three-dimensional.

Based on the wind pressure distributions around building models, when the U1, U2 and, U7, U8 models are compared, it is seen that the negative pressure difference decreases slightly as the depth ratio decreases. Besides, as the wind velocity increased, the negative pressure difference decreased. It was observed that there was no significant difference in terms of positive pressure values (Tables 2–3).

Table 2 Comparison of pressures according to the wind velocity changes

	DR	V	Positive Pressure (P)	Negative Pressure (N)
U1	4	2		
U2	4	5	$8 \times U1$	$11 \times U1$
U7	0.5	2		
U8	0.5	5	$8 \times U7$	$6 \times U7$

Table 3 Comparison of pressures according to the depth ratio changes

	DR	V	Positive Pressure (<i>P</i>)	Negative Pressure (<i>N</i>)
U1	4	2		
U7	0.5	5	similar with U1	$2 \times U1$
U2	4	2		
U8	0.5	5	similar with U2	$1.5 \times U2$

When the models U1 and U2, which have the same depth ratio of 4, were compared, it was observed that positive pressure values around the U2 model, which was exposed to 5 m/s wind velocity, are approximately eight times that of the U1 model. Besides this, negative pressure values are about 11 times greater than U1. When the models U1 and U7, which were exposed to 2 m/s wind velocity, were compared, it was observed that there was no significant difference in terms of positive pressure values. However, significant differences were observed in negative pressure values. It has been observed that the negative pressure

values around the U7 model – depth ratio 0.5 – are approximately twice that of the U1 model with a depth ratio of 4. The higher pressure changes were noticed in these models.

Based on the velocity distributions, the vortex region becomes smaller from the height levels of $H/3$ to $2H/3$. This vortex area is larger in the U7 model, with a depth ratio of 0.5. The vortex area gets more prominent as the depth ratio decreases. In the trace region, velocity decreases in all models in the velocity region. However, as the height of the model decreases, the velocity drops in the track zone increases. When the models of U1 and U2, which were exposed to the same depth ratio and different wind velocities, were compared, it was noticed that the U2 model had considerable high-pressure values. Moreover, while the pressure areas on the side surfaces of the U2 and U8 models, which are exposed to high wind velocity, decrease with height, an increasing trend is observed for U1 and U7, which are exposed to low wind velocity.

References

- Al-Najjar, S. F., Al-Azhari, W. W. (2021) "Review of Aerodynamic Design Configurations for Wind Mitigation in High-Rise Buildings: Two Cases from Amman", *Civil Engineering and Architecture*, 9(3), pp. 708–720.
<https://doi.org/10.13189/cea.2021.090313>
- Bhattacharya, B., Dalui S. K. (2020) "Experimental and Numerical Study of Wind-Pressure Distribution on Irregular-Plan-Shaped Building", *Journal of Structural Engineering*, 146(7), pp. 1–14.
[https://doi.org/10.1061/\(ASCE\)ST.1943-541X.0002686](https://doi.org/10.1061/(ASCE)ST.1943-541X.0002686)
- Bhattacharyya, B., Dalui, S. K. (2018) "Investigation of mean wind pressures on 'E' plan-shaped tall building", *Wind and Structures*, 26(2), pp. 99–114.
<https://doi.org/10.12989/was.2018.26.2.099>
- Chakraborty, S., Dalui, S. K., Ahuja, A. K. (2014) "Wind load on irregular plan-shaped tall building - a case study", *Wind and Structures*, 19(1), pp. 59–73.
<https://doi.org/10.12989/was.2014.19.1.059>
- Franke, J. (2006) "Recommendations of the Cost Action C14 on the use of CFD in Predicting Pedestrian Wind Environment", In: Fourth International Symposium on Computational Wind Engineering (CWE2006), Yokohama, Japan, pp. 529–532.
- Gomes, M. G., Rodrigues, A. M., Mendes, P. (2005) "Experimental and numerical study of wind pressures on irregular-plan shapes", *Journal of Wind Engineering and Industrial Aerodynamics*, 93, pp. 741–756.
<https://doi.org/10.1016/j.jweia.2005.08.008>
- Inan, T. (2021) "Wind Flow Analysis on Simple Plan-Shaped Buildings", *Megaron*, 16(2), pp. 286–305.
<https://doi.org/10.14744/MEGARON.2021.99975>
- Jendzelovsky, N., Antal, R. (2021) "CFD and Experimental Study of Wind Pressure Distribution on the High-Rise Building in the Shape of an Equilateral Acute Triangle", *Fluids*, 6(2), 81.
<https://doi.org/10.3390/fluids6020081>
- Li, Y., Duan, R.-B., Li, Q.-S., Li, Y.-G., Li, C. (2020) "Research on the characteristics of wind pressures on L-shaped tall buildings", *Advances in Structural Engineering*, 23(10), pp. 2070–2085.
<https://doi.org/10.1177/1369433220906934>
- Mallick, M., Kumar, A., Patra, K. C. (2019) "Experimental Investigation on the Wind-Induced Pressures on C-Shaped Buildings", *KSCE Journal of Civil Engineering*, 23, pp. 3535–3546.
<https://doi.org/10.1007/s12205-019-1929-6>
- Mallick, M., A., Mohanta, A., Kumar, K., Patra, K. C. (2020) "Gene-expression programming for the assessment of surface mean pressure coefficient on building surfaces", *Building Simulation*, 13, pp. 401–418.
<https://doi.org/10.1007/s12273-019-0583-8>
- Mukherjee, S., Chakraborty, S., Dalui, S. K., Ahuja, A. K. (2014) "Wind induced pressure on Y plan shape tall building", *Wind and Structures*, 19(5), pp. 523–540.
<https://doi.org/10.12989/was.2014.19.5.523>
- Patankar, S. V. (1980) "Numerical Heat Transfer and Fluid Flow", Hemisphere Publishing, Washington, DC, USA. ISBN 0070487405
- Paul, R., Dalui, S. K. (2021) "Shape Optimization to Reduce Wind Pressure on the Surfaces of a Rectangular Building with Horizontal Limbs", *Periodica Polytechnica Civil Engineering*, 65(1), pp. 134–149.
<https://doi.org/10.3311/PPci.16888>
- Sanyal, P., Dalui, S. K. (2021) "Effects of internal angle between limbs of 'Y' plan shaped tall building under wind load", *Journal of Building Engineering*, 33, 101843.
<https://doi.org/10.1016/j.jobbe.2020.101843>
- Tominaga, Y., Mochida, A., Yoshie, R., Kataoka, H., Nozu, T., Yoshikawa, M., Shirasawa, T. (2008) "AIJ Guidelines for Practical Applications of CFD to Pedestrian Wind Environment around Buildings", *Journal of Wind Engineering and Industrial Aerodynamic*, 96, pp. 1749–1761.
<https://doi.org/10.1016/j.jweia.2008.02.058>